Numerical investigation on the fixed-stress splitting scheme for Biot's equations: Optimality of the tuning parameter

Jakub W. Both[1] and Uwe Köcher[2]

[1] University of Bergen, Bergen, Norway, jakub.both@uib.no
[2] Helmut-Schmidt-University, University of the Federal Armed Forces Hamburg, Germany, uwe.koecher@hsu-hh.de

Abstract. We study the numerical solution of the quasi-static linear Biot equations solved iteratively by the fixed-stress splitting scheme. In each iteration the mechanical and flow problems are decoupled, where the flow problem is solved by keeping an artificial mean stress fixed. This introduces a numerical tuning parameter which can be optimized. We investigate numerically the optimality of the parameter and compare our results with physically and mathematically motivated values from the literature, which commonly only depend on mechanical material parameters. We demonstrate, that the optimal value of the tuning parameter is also affected by the boundary conditions and material parameters associated to the fluid flow problem suggesting the need for the integration of those in further mathematical analyses optimizing the tuning parameter.

1 Introduction

The coupling of mechanical deformation and fluid flow in porous media is relevant in many applications ranging from environmental to biomedical engineering. In this paper, we consider the simplest possible fully coupled model given by the quasi-static Biot equations [3], coupling classical and well-studied subproblems from linear elasticity and single phase flow in fully saturated porous media. Due to the complex structure of the coupled problem, the development of monolithic solvers is not trivial and topic of current research. Hence, instead of developing new simulation tools for the coupled problem, due to their simplicity and flexibility, splitting methods have been very attractive recently allowing the use of independent, tailored simulators for both subproblems. Among various iterative splitting schemes, one of the most prominent schemes is the physically motivated fixed-stress splitting scheme [8], based on solving sequentially the mechanics and flow problems while keeping an artificial mean stress fixed in the latter. From an abstract point of view, the splitting scheme is a linearization scheme employing positive pressure stabilization, a concept also applied for the linearization of other problems as, e.g., the Richards equation [5]. Addressing the physical formulation, the definition of the artificial mean stress includes a user-defined tuning parameter. It can be chosen *a priori* such that the resulting fixed-stress splitting scheme is unconditionally stable in the sense of a von Neumann stability analysis [6] and it is globally contractive [1,2,4,7]. Suggested values for the tuning parameter from literature are either physically motivated [6] or mathematically motivated [1,2,4,7]. The latter works prove theoretically global contraction of the scheme, allowing to optimize the resulting theoretical contraction rate, and hence, proposing a value for the tuning parameter with suggested, better performance than for the physically motivated parameters. In general, the suggested values for the tuning parameter given in the literature do not necessarily yield a minimal number of iterations, which for strongly coupled problems is crucial. For increasing coupling strength the problem becomes more difficult to solve, and the performance of the fixed-stress splitting scheme is very sensitive to the choice of the tuning parameter. The mentioned tuning parameters depend solely on mechanical material parameters. However, practically, it is known that the physical character of the problem governed by boundary conditions also affects the performance of the scheme [6], introducing the main difficulty finding an optimal tuning parameter. We note that the fixed-stress splitting scheme can also be applied as a preconditioner for Krylov subspace methods solving Biot's equation in a monolithic fashion. In this case, performance is less sensitive with respect to the tuning parameter.

In this work, we investigate numerically whether the optimal tuning parameter obtained by simple trial and error is closer related to the mathematically or the physically motivated parameters. Furthermore, we investigate whether the optimal tuning parameter is also dependent on more than only mechanical properties. For this purpose, we perform a numerical study enhancing a test case from [1] and measure performance of the fixed-stress splitting scheme for different tuning parameters. Our main results are:

- Boundary conditions affect the optimality of the tuning parameter.
- Fluid flow parameters affect the optimality of the tuning parameter.
- Both should be included in the mathematical analysis allowing to derive theoretically an optimal tuning parameter.

2 Linear Biot's equations

We consider the quasi-static Biot equations [3], modeling fluid flow in a deformable, linearly elastic porous medium $\Omega \subset \mathbb{R}^d$, $d \in \{1,2,3\}$, fully saturated by a slightly compressible fluid. Using mechanical displacement $\boldsymbol{u}$, fluid pressure p and fluid flux $\boldsymbol{q}$ as primary variables, on the space-time domain $\Omega \times (0,T)$, the governing equations written in a three-field formulation read

$$-\boldsymbol{\nabla} \cdot (2\mu\boldsymbol{\varepsilon}(\boldsymbol{u}) + \lambda \boldsymbol{\nabla} \cdot \boldsymbol{u}\boldsymbol{I} - \alpha p \boldsymbol{I}) = \rho_{\mathrm{b}} \boldsymbol{g}, \tag{1}$$

$$\partial_t \left(\frac{p}{M} + \alpha \boldsymbol{\nabla} \cdot \boldsymbol{u} \right) + \boldsymbol{\nabla} \cdot \boldsymbol{q} = 0, \tag{2}$$

$$\frac{\eta}{k} \boldsymbol{q} + \boldsymbol{\nabla} p = \rho_{\mathrm{f}} \boldsymbol{g}. \tag{3}$$

Eq. (1) describes balance of momentum at each time, Eq. (2) describes mass conservation and Eq. (3) describes Darcy's law. Here, $\boldsymbol{\varepsilon}(\boldsymbol{u}) = \frac{1}{2}\left(\boldsymbol{\nabla}\boldsymbol{u} + \boldsymbol{\nabla}\boldsymbol{u}^\top\right)$ is the linearized strain tensor, μ, λ are the Lamé parameters (equivalent to Young's modulus E and Poisson's ratio ν via $\mu = \frac{E}{2(1+\nu)}$ and $\lambda = \frac{E\nu}{(1+\nu)(1-2\nu)}$), α is the Biot coefficient, M is the Biot modulus, ρ_f is the fluid density, ρ_b is the bulk density, k is the absolute permeability, η the fluid viscosity and $\boldsymbol{g}$ is the gravity vector. In this work, we assume isotropic, homogeneous materials, i.e., all material parameters are constants.

The system (1)–(3) is closed by postulating initial conditions $\boldsymbol{u} = \boldsymbol{u}_0$, $p = p_0$ on $\Omega \times \{0\}$, satisfying Eq. (1), and boundary conditions $\boldsymbol{u} = \boldsymbol{u}_\mathrm{D}$ on $\Gamma_{\mathrm{D,m}} \times (0,T)$, $(2\mu\boldsymbol{\varepsilon}(\boldsymbol{u}) + \lambda\boldsymbol{\nabla}\cdot\boldsymbol{u}\boldsymbol{I} - \alpha p\boldsymbol{I})\cdot\boldsymbol{n} = \boldsymbol{\sigma}_\mathrm{N}$ on $\Gamma_{\mathrm{N,m}} \times (0,T)$, $p = p_\mathrm{D}$ on $\Gamma_{\mathrm{D,f}} \times (0,T)$, $\boldsymbol{q}\cdot\boldsymbol{n} = q_\mathrm{N}$ on $\Gamma_{\mathrm{N,f}} \times (0,T)$ on partitions $\Gamma_{\mathrm{D},\star} \cup \Gamma_{\mathrm{N},\star} = \partial\Omega$, $\star \in \{m, f\}$, where $\boldsymbol{n}$ is the outer normal on $\partial\Omega$.

Here and in the remaining paper, we omit introducing a corresponding variational formulation and suitable function spaces, as they appear naturally. For details, we refer to our works [1,4].

3 Fixed-stress splitting scheme

We solve the coupled Biot equations (1)–(3) iteratively using the fixed-stress splitting scheme [8], which decouples the mechanics and fluid flow problems. Each iteration, defining the approximate solution $(\boldsymbol{u}, p, \boldsymbol{q})^i$, $i \in \mathbb{N}$, consists of two steps. First, the flow problem is solved assuming a fixed artificial, volumetric stress $\sigma_v = K_\mathrm{dr}\boldsymbol{\nabla}\cdot\boldsymbol{u} - \alpha p$, where K_dr is a tuning parameter, which will be discussed in the scope of this paper: Given $(\boldsymbol{u}, p, \boldsymbol{q})^{i-1}$, find $(p, \boldsymbol{q})^i$ satisfying

$$\left(\frac{1}{M} + \frac{\alpha^2}{K_\mathrm{dr}}\right)\partial_t p^i + \boldsymbol{\nabla}\cdot\boldsymbol{q}^i = \frac{\alpha^2}{K_\mathrm{dr}}\partial_t p^{i-1} - \alpha\partial_t\boldsymbol{\nabla}\cdot\boldsymbol{u}^{i-1}, \tag{4}$$

$$\frac{\eta}{k}\boldsymbol{q}^i + \boldsymbol{\nabla}p^i = \rho_\mathrm{f}\boldsymbol{g}, \tag{5}$$

including corresponding initial and boundary conditions. Second the mechanics problem is solved with updated flow fields: Find $\boldsymbol{u}^i$ satisfying corresponding boundary conditions and

$$-\boldsymbol{\nabla}\cdot\left(2\mu\boldsymbol{\varepsilon}(\boldsymbol{u}^i) + \lambda\boldsymbol{\nabla}\cdot\boldsymbol{u}^i\boldsymbol{I} - \alpha p^i\boldsymbol{I}\right) = \rho_\mathrm{b}\boldsymbol{g}. \tag{6}$$

The tuning parameter K_dr

The fixed stress splitting scheme can be interpreted as a two block Gauss-Seidel method with an educated predictor for mechanical displacement used in the solution of the flow problem. More precisely, the mechanics problem (1) is solved inexactly for the volumetric deformation by reduction to the one-dimensional equation

$$K_\mathrm{dr}\boldsymbol{\nabla}\cdot(\boldsymbol{u}^i - \boldsymbol{u}^{i-1}) - \alpha(p^i - p^{i-1}) = 0 \tag{7}$$

and inserted into the flow equation (2). In the special case of nearly incompressible materials, i.e., $\mu/\lambda \to 0$ or $\nu \to 0.5$, Eq. (1) yields $\boldsymbol{\nabla}\partial_t(\lambda\boldsymbol{\nabla}\cdot\boldsymbol{u}-\alpha p) \approx \mathbf{0}$. Hence, we expect the ansatz (7) to be nearly exact for $K_{\mathrm{dr}} = \lambda$, yielding a suitable tuning parameter for nearly incompressible materials.

An exact inversion of Eq. (1) for the volumetric deformation would be given by the divergence of a Green's function and thus would be defined locally and depend on fluid pressure, geometry, material parameters and boundary conditions, both associated with the mechanical subproblem. However, due to lack of *a priori* knowledge and simplicity, in the literature, the considered inexact inversion includes only fluid pressure and mechanical material parameters introduced via the tuning parameter K_{dr}. Selected values are $K_{\mathrm{dr}}^{1\mathrm{D}}$, $K_{\mathrm{dr}}^{2\mathrm{D}}$ $K_{\mathrm{dr}}^{3\mathrm{D}}$, cf. [6], $K_{\mathrm{dr}}^{2\times\lambda}$, cf. [1,2,7], and $K_{\mathrm{dr}}^{2\times d\mathrm{D}}$, cf. [4,7], defined by

$$K_{\mathrm{dr}}^{d^\star\mathrm{D}} = \frac{2\mu}{d^\star} + \lambda,\ d^\star \in \{1,2,3\}, \qquad K_{\mathrm{dr}}^{2\times\lambda} = 2\lambda, \qquad K_{\mathrm{dr}}^{2\times d\mathrm{D}} = 2\, K_{\mathrm{dr}}^{d\mathrm{D}}.$$

The choice $K_{\mathrm{dr}}^{d^\star\mathrm{D}}$ is purely physically motivated and equals the bulk modulus of a $d^\star$-dimensional material. Independent of the spatial dimension d, for uniaxial compression, biaxial compression or general deformations, we choose $d^\star = 1, 2, 3$, respectively. Following [6], if not known better *a priori*, choose $d^\star = d$. Eq. (7) with $K_{\mathrm{dr}} = K_{\mathrm{dr}}^{d\mathrm{D}}$ corresponds to fixing the trace of the physical, poroelastic stress tensor. The choices $K_{\mathrm{dr}}^{2\times\lambda}$ and $K_{\mathrm{dr}}^{2\times d\mathrm{D}}$ have resulted from optimization of the obtained theoretical contraction rate. Those analyses have in common that global convergence is guaranteed for $0 \leq K_{\mathrm{dr}} \leq K_{\mathrm{dr}}^{2\times\lambda}$ and $0 \leq K_{\mathrm{dr}} \leq K_{\mathrm{dr}}^{2\times d\mathrm{D}}$, hence, the latter also covers convergence for the physical choices. Additionally, the analyses indicate that the larger K_{dr} the faster convergence, suggesting that the mathematically motivated parameters should yield better performance than the physically motivated parameters. In the following section we investigate this statement numerically.

4 Numerical study – Optimal tuning parameter K_{dr}

We perform a numerical parameter study analyzing the optimality of the tuning parameter K_{dr} in the view of the performance of the fixed-stress splitting scheme measured in terms of number of fixed-stress iterations. Inspired by a test setting from [1], we consider four test cases based on an L-shaped domain $\Omega = (-0.5, 0.5)^2 \setminus [0, 0.5]^2 \subset \mathbb{R}^2$ in the time interval $(0, 0.5)$ under two sets of boundary conditions, identified by test cases 1a/b/c, and test case 2, cf. Fig. 1. For all cases, vanishing initial conditions $p_0 = 0$ and $\boldsymbol{u}_0 = \mathbf{0}$ are prescribed. A traction $\boldsymbol{\sigma}_{\mathrm{N}}(t) = (0, -h_{\max} \cdot 256 \cdot t^2 \cdot (t - 0.5)^2)$ is applied on the top with $h_{\max}$ suitably chosen. Additionally, we prescribe $p_{\mathrm{D}} = 0$ on the top and $q_{\mathrm{N}} = 0$ on the remaining boundary, zero normal displacement and homogeneous tangential traction on the left and bottom side, and a homogeneous traction on the lower right side. In the test cases 1a/b/c, we also prescribe zero normal displacement on the cut, whereas in test case 2, a homogeneous traction is applied on the cut. The different sets of boundary conditions result in two different physical scenarios. Despite the two-dimensional, non-symmetric geometry, the test cases 1a/b/c are closely related to a classical uniaxial compression, whereas the second test case describes a true two-dimensional deformation.

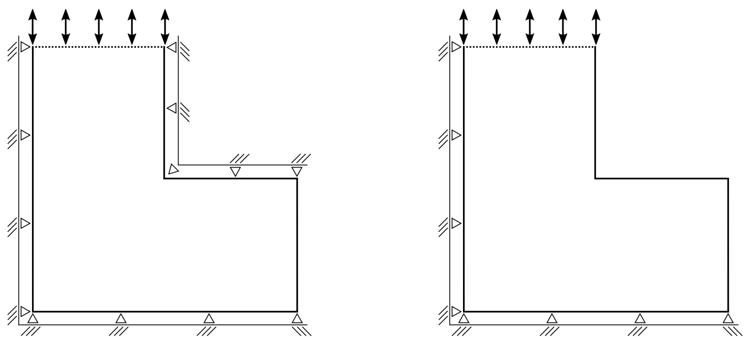

(a) Test cases 1a/b/c. (b) Test case 2.

Fig. 1: Geometry and boundary conditions employed in the numerical study.

For the numerical discretization of Eq. (1)–(3) in space we use piecewise linear, piecewise constant and lowest order Raviart-Thomas finite elements for $\boldsymbol{u}$, p and $\boldsymbol{q}$, respectively, defined on a structured, quadrilateral mesh with 16 elements per x- and y-direction. Additionally, for the time discretization we use the backward Euler method with a fixed time step size $\Delta t = 0.01$. We solve the discretized Eq. (1)–(3) using the fixed-stress splitting scheme (4)–(6) for a range of tuning parameters $K_{\mathrm{dr}} = \omega K_{\mathrm{dr}}^{\mathrm{1D}}$ for test cases 1a/b/c and $K_{\mathrm{dr}} = \omega K_{\mathrm{dr}}^{\mathrm{2D}}$ for test case 2, $\omega \in \{0.5, 0.51, ..., 1.3\}$, and present the accumulated number of iterations required for convergence of the fixed-stress splitting scheme. In the following, we denote $K_{\mathrm{dr}}^{\star}$ to be the K_{dr} yielding minimal number of iterations for a single test case. As stopping criterion, we employ the discrete Euclidean norm $\| \cdot \|_{l^2}$ for the algebraic increments between two successive solution vectors for each of the unknown variables $\boldsymbol{u}$, p and $\boldsymbol{q}$. The numerical examples are implemented using the deal.II library (and are verified by an implementation using the DUNE library).

Test case 1a – Effective 1d deformation

We consider a fixed Young's modulus $E = 100$ [GPa] and a varying Poisson's ratio $\nu \in \{0.01, 0.1, 0.2, 0.3, 0.4, 0.49\}$. Moreover, we fix $k = 100$ [mD], $\eta = 1$ [cP], $\alpha = 0.9$, $M = 100$ [GPa], $\boldsymbol{g} = \boldsymbol{0}$ [m/s^2]. On top, we apply the normal force $\boldsymbol{\sigma}_{\mathrm{N}}$ with $h_{\max} = 10$ [GPa]. The number of required fixed stress iterations in relation to the tuning parameter is displayed in Fig. 2a. Here, the choice

$K_{\mathrm{dr}} = K_{\mathrm{dr}}^{\mathrm{1D}}$ is suitable independent of the Poisson ratio, confirming that the problem is essentially driven by uniaxial compression.

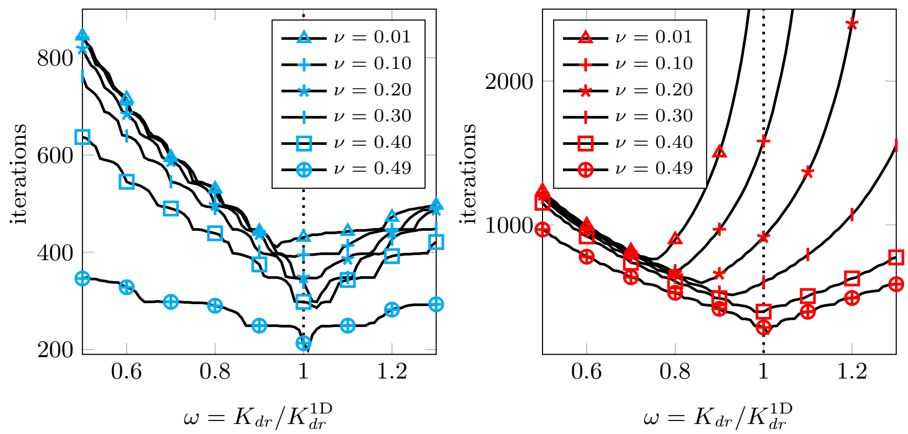

(a) Test case 1a ($E = 100$ GPa). (b) Test case 1b ($E = 1$ GPa).

Fig. 2: Total number of fixed stress iterations vs. tuning parameter.

Test case 1b – Soft material

We modify test case 1a and consider now a softer material with Young's modulus $E = 1$ [GPa], yielding a stronger coupling of the mechanics and flow problem. On top, we apply the normal force $h_{\max} = 0.1$ [GPa], resulting in a comparable maximal displacement of the top boundary. Apart from that, we use the same parameters as in test case 1a. The number of required fixed stress iterations in relation to the tuning parameter is displayed in Fig. 2b. Compared to the previous test case, the nature of the mechanical problem becomes more two-dimensional, indicated by $K_{\mathrm{dr}}^{\star}$ lying between $K_{\mathrm{dr}}^{\mathrm{1D}}$ and $K_{\mathrm{dr}}^{\mathrm{2D}}$. More precisely, $K_{\mathrm{dr}}^{\star}/K_{\mathrm{dr}}^{\mathrm{1D}}$ depends on ν. Only for nearly incompressible materials $K_{\mathrm{dr}} = K_{\mathrm{dr}}^{\mathrm{1D}} \approx K_{\mathrm{dr}}^{\mathrm{2D}}$ is a suitable choice. Hence, we see that the mechanical character of the problem can vary with changing material parameters but fixed boundary conditions.

Test case 1c – Influence of flow parameter

We consider a particular example of test case 1b ($E = 1$ [GPa], $\nu = 0.01$) for varying permeability $k \in \{1e\text{-}1, 1e0, ..., 1e3\}$ [mD]. Apart from that, we use the same parameters as in test case 1b. The number of required fixed stress iterations in relation to the tuning parameter is displayed in Fig. 3a. We observe that although all possible mechanical input data is fixed (mechanical boundary conditions and material parameters), the optimal tuning parameter $K_{\mathrm{dr}}^{\star}$ is in general also dependent on material parameters associated with the flow problem. In particular, for decreasing permeability, the optimal $K_{\mathrm{dr}}^{\star}$ increases towards $K_{\mathrm{dr}}^{1,\mathrm{D}}$.

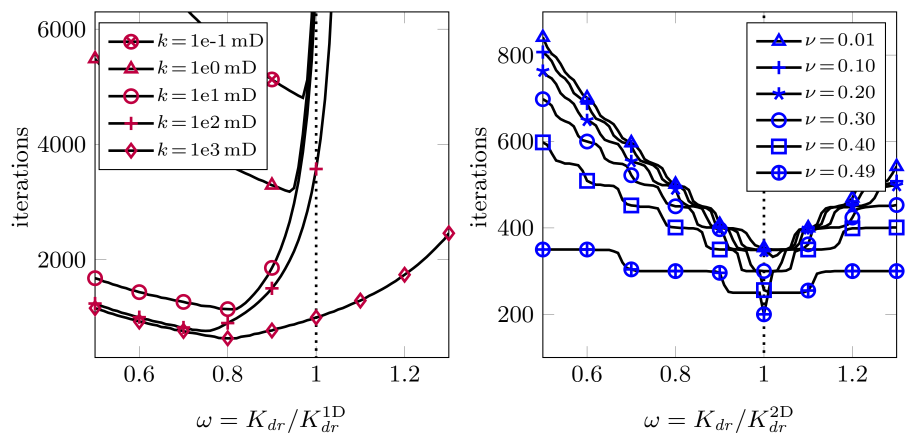

(a) Test case 1c ($E = 1$ GPa, $\nu = 0.01$). (b) Test case 2 ($E = 100$ GPa).

Fig. 3: Total number of fixed stress iterations vs. tuning parameter.

Test case 2 – True 2d deformation

We consider test case 2 with same parameters as in test case 1a, changing only from Dirichlet to Neumann boundary conditions on single parts of the boundary. The number of required fixed stress iterations in relation to the tuning parameter is displayed in Fig. 3b. We observe that the optimal tuning parameter $K_{\mathrm{dr}}^{\star}$ is essentially equal to $K_{\mathrm{dr}}^{2\mathrm{D}}$, indicating that, the boundary conditions generate a true two-dimensional deformation and determine fully the optimal tuning parameter $K_{\mathrm{dr}}^{\star}$.

5 Conclusion

In general, the *a priori* choice of an optimal tuning parameter $K_{\mathrm{dr}}^{\star}$ is not trivial. It is depending on the coupling strength which itself depends on various material and discretization parameters. In the above test cases we have observed:

- The mathematically motivated tuning parameters $K_{\mathrm{dr}}^{2\times\lambda}$ and $K_{\mathrm{dr}}^{2\times 2\mathrm{D}}$ have in general not in the slightest shown to be optimal, which can be confirmed without difficulty for e.g. nearly incompressible materials. Instead,

the optimal $K_{\mathrm{dr}}^{\star}$ has been closer related to the physically motivated parameters $K_{\mathrm{dr}}^{d^{\star}\mathrm{D}}$.
- Mechanical boundary conditions are able to determine essentially the physics and define the optimal $K_{\mathrm{dr}}^{\star}$, cf. test case 1a/2, which is consistent with [6]. However, they do not necessarily solely determine the optimal $K_{\mathrm{dr}}^{\star}$, cf. test case 1b. Furthermore, although the fixed-stress approach is based on the inexact inversion of the mechanics equation (1), also fluid flow properties can influence $K_{\mathrm{dr}}^{\star}$, cf. test case 1c. We note, that in general one can expect a further dependence on the domain and boundary size, which has not been studied here.
- As expected, for nearly incompressible materials, a suitable tuning parameter is given by $K_{\mathrm{dr}} = \lambda \approx K_{\mathrm{dr}}^{d^{\star}\mathrm{D}} \approx \frac{1}{2} K_{\mathrm{dr}}^{2\times\lambda} \approx \frac{1}{2} K_{\mathrm{dr}}^{2\times 2\mathrm{D}}$, cf. Section 3.

All in all, the optimal tuning parameter $K_{\mathrm{dr}}^{\star}$ does not solely depend on the Lamé parameters, but also other physical material parameters, the physical character of the problem and numerical discretization parameters. The latter has been also studied in [1]. All in all, future theoretical analysis of $K_{\mathrm{dr}}^{\star}$ should also include the effect of those additional parameters. However, in practice, we expect the dependence of $K_{\mathrm{dr}}^{\star}$ on the input data of the problem to be complex, and therefore plan to investigate adaptive techniques for determining a locally defined approximation of $K_{\mathrm{dr}}^{\star}$.

Acknowledgments

The research contribution of the second author was partially supported by E.ON Stipendienfonds (Germany) under the grant T0087 29890 17 while visiting University of Bergen.

References

1. M. Bause, F. Radu, U. Köcher, *Space-time finite element approximation of the Biot poroelasticity system with iterative coupling*, Comput. Methods Appl. Mech. Engrg., **320** (2017), 745–768.
2. M. Bause, *Iterative coupling of mixed and discontinuous Galerkin methods for poroelasticity*, ENUMATH 2017 Proceedings, **submitted**.
3. M.A. Biot, *General theory of three-dimensional consolidation*, J. Appl. Phys. **12** (1941), 155–164.
4. J.W. Both, M. Borregales, J.M. Nordbotten, K. Kumar, F.A. Radu, *Robust fixed stress splitting for Biot's equations in heterogeneous media*, Appl. Math. Lett. **68** (2017), 101–108.
5. F. List, F.A. Radu, *A study on iterative methods for solving Richards' equation*, Comput. Geosci. **20** (2016), pp. 341–353.
6. J. Kim, H.A. Tchelepi, R. Juanes, *Stability and convergence of sequential methods for coupled flow and geomechanics: Fixed-stress and fixed-strain splits*, Comput. Methods Appl. Mech. Engrg., **200** (2011), 1591–1606.

7. A. Mikelić, M.F. Wheeler, *Convergence of iterative coupling for coupled flow and geomechanics*, Comput. Geosci. **17** (2013), 451–461.

8. A. Settari, F.M. Mourits, *A coupled reservoir and geomechanical simulation system*, Soc. Pet. Engrg. J., **3** (1998), pp. 219–226.